



# Terminator Double Layer Explorer (TerDLE): Examining the Near-Moon Lunar Wake

W. M. Farrell<sup>1</sup>, P. E. Clark<sup>2</sup>, M. R. Collier<sup>1</sup>, B. Malphrus<sup>3</sup>, D. C. Folta<sup>1</sup>, M. Keidar<sup>4</sup>, D. C. Bradley<sup>1</sup>, R. J. MacDowall<sup>1</sup>, and J. W. Keller<sup>1</sup>

<sup>1</sup>NASA/Goddard Space Flight Center, Greenbelt, MD, USA

<sup>2</sup>NASA/Jet Propulsion Laboratory, Pasadena, CA, USA

<sup>3</sup>Morehead State University, Morehead, KY, USA

<sup>4</sup>George Washington University, Washington, DC 012121, USA

Received 2020 October 20; revised 2020 December 30; accepted 2021 January 19; published 2021 March 18

## Abstract

As the solar wind flows by the Moon, an antisunward-directed low-density wake forms as the plasma expands to fill in the trailing void in the plasma flow. Analytical modeling and modern plasma simulations suggest that plasma quasi-neutrality could possibly be broken close to the terminator obstruction as solar wind electrons expand into the wake ahead of the ions, leading to the formation of a standing (time-stationary) double layer. The objective of the Terminator Double Layer Explorer is to extend the fundamental understanding of the plasma expansion into the trailing near-vacuum wake region by (1) identifying any plasma expansion density anomalies at low altitudes near the terminator wake initiation region, (2) assessing the highly variable solar wind's effect on the low-altitude wake region, and (3) determining if plasma neutrality is maintained or lost during passages through the low-altitude expansion region. The mission concept uses a propulsion-driven CubeSat with ion spectrometer and plasma wave system in elliptical orbit about the Moon with periselene near the terminator. Over the course of the mission, the periselene decreases, placing the CubeSat ever closer to the terminator wake initiation location and the possible nonneutral region.

*Unified Astronomy Thesaurus concepts:* [Lunar science \(972\)](#); [Plasma physics \(2089\)](#); [Space plasmas \(1544\)](#)

## 1. Introduction

The Moon is an obstacle to the antisunward-flowing solar wind plasma, and a substantial plasma perturbation trails the body to over 17,000 km (or 10 lunar radii,  $R_L$ ) downstream (Farrell et al. 1998, 2002). The conventional wisdom is that the Moon absorbs nearly 100% of the incident solar wind on the dayside, thereby leaving a trailing plasma void—almost a near-perfect vacuum—in its wake. Early exploration of the lunar space environment by spacecraft like Explorer-35 and Apollo subsatellites focused on the unexpected and complicated magnetic signature in the trailing wake region (Ness et al. 1968; Ness & Schatten 1969; Ness 1972; Schubert & Lichtenstein 1974). The plasma–vacuum interface (i.e., the wake flank) was described as an extended magnetohydrodynamic tangential discontinuity that disallowed solar wind ion inflow in regions antisunward of the Moon (Spreiter et al. 1970).

Serendipitously, a new view of the lunar wake resulted when the Wind spacecraft made transits at a few lunar radii downstream (for trajectory maneuvers). During these passages, the wake was investigated with modern plasma ion and electron spectrometers (Bosqued et al. 1996; Ogilvie et al. 1996), magnetometers (Farrell et al. 1996; Owens et al. 1996), and plasma wave systems (Bale et al. 1997; Farrell et al. 1997). The observations were extraordinary, finding that the ions do indeed expand into the trailing wake region via a plasma expansion process similar to that found trailing the space shuttle in the ionospheric plasma (Tribble 1988; Tribble et al. 1989).

Specifically, at the plasma–vacuum interface, energetic electrons are thought to propagate into the void ahead of the more massive ions and, in doing so, create an expansion  $E$ -field that deflects the ion flow into the void. The ions become accelerated by this  $E$ -field to form ion beams (Samir et al. 1983; Ogilvie et al. 1996). For a magnetic field line crossing the cylindrical wake structure, counterstreaming ion beams are launched from the edges of the void; these are flowing toward the central wake region along the threading magnetic field lines (Ogilvie et al. 1996; Clack et al. 2004; Halekas et al. 2011). These counterstreaming ion flows were also found to be the source of intense ion–ion plasma wave activity (Farrell et al. 1997, 1998).

In the late 1990s/early 2000s, the Lunar Prospector (LP) spacecraft made over 6000 passes through the wake region from 115 km to as low as 20 km altitude. Halekas et al. (2005) showed that the observations, both as an ensemble and in individual passes, were consistent with a plasma expansion of a kappa distribution of electrons flowing into the trailing void. Unfortunately, there were no corresponding ion observations, and the lack of ion observations of the expansion is a reason to revisit this near-Moon region with the Terminator Double Layer Explorer (TerDLE).

In the late 2000s, plasma instrumentation on board Japan's Kaguya spacecraft also observed the plasma expansion but also reported on a “type II wake” that was found in about 5%–10% of near-Moon wake crossings (Nishino et al. 2010). Specifically, dayside reflected solar wind protons (Saito et al. 2008) could perform a circular trajectory about the local magnetic field, taking these ions directly into the trailing wake. In doing so, a proton-governed region (PGR) is formed that creates an  $E$ -field that accelerates electrons into the wake. In this case, near the PGR, the  $E$ -field is directed opposite to the normal expansion process and causes the near-Moon electrons to accelerate into the void.



Original content from this work may be used under the terms of the [Creative Commons Attribution 4.0 licence](#). Any further distribution of this work must maintain attribution to the author(s) and the title of the work, journal citation and DOI.

The twin THEMIS-ARTEMIS spacecraft are currently in orbit about the Moon making key measurements of pickup ions (Halekas et al. 2012), unusual wake geometries (for example, Poppe et al. 2014) and the overall wake structure (Halekas et al. 2014; Zhang et al. 2014, 2016; Xu et al. 2019). One spacecraft is traveling prograde and the other retrograde about the Moon, and both are in  $\sim 100$  by 19,000 km low-inclination orbits (Angelopoulos et al. 2011). Both THEMIS-ARTEMIS spacecraft have an ion spectrometer (IS), electron spectrometer, and plasma wave system (PWS; Bonnell et al. 2008; McFadden et al. 2008). The local time of periselene will vary, and only occasionally will it occur just nightside of the terminator. To date, there have been no systematic THEMIS-ARTEMIS studies of the near-Moon wake flank—the wake initiation region—just downstream of the terminator, especially examining a large set of passes just nightside of the terminator.

We thus describe herein a CubeSat concept called TerDLE that explores the lunar wake region at very low altitudes—in regions just downstream of the terminator obstacle—to examine the early evolution of the plasma flow into the trailing void. TerDLE will also search for a nonneutral region called a double layer (i.e., adjacent oppositely charged plasma regions) that might form immediately downstream of the terminator. Section 2 further describes the expected near-Moon plasma discontinuity at the terminator. Section 3 provides the TerDLE mission objectives, and Section 4 provides a brief description of the TerDLE instruments. Section 5 describes the TerDLE implementation as a 12 kg/6U CubeSat, while Section 6 describes enhancements to the mission, including other instruments that could be accommodated on a larger bus to enhance the science.

We note that TerDLE was submitted as a proposal to the 2014 NASA/Heliophysics Technology and Instrument Development for Science (H-TiDeS) solicitation and, as a payload, was required to fit in a 12 kg/6U CubeSat bus to be carried as a deployable package on board Artemis-1. We thus describe the mission concept in this limited context in Section 5 but fully realize that a larger spacecraft with added complementary instruments could also target this same objective. Thus, alternate scenarios for a larger system will be described in Section 6.

## 2. The Near-Moon Plasma–Vacuum Discontinuity

Consider the development of a time-stationary near-perfect plasma–vacuum discontinuity like that which would form just downstream of the lunar terminator. It would be limited in downstream extent but should form an annulus about the entire terminator.

The plasma expansion in this initiation region should be a near-perfect discontinuity. However, there are two different views of the early expansion period, depending upon the initial assumptions. Analytical formalism appears in the literature that solves the fluid equations by initially setting the electron and ion density to be equal (quasi-neutrality; see review by Samir et al. 1983). Applications using hybrid plasma simulations also fix plasma neutrality (the ion densities equal the electron densities,  $n_i = n_e$ ). In doing so, the ions expand into the void in concentrations identical to the electrons.

However, Crow et al. (1975) also used the fluid equations to derive the expansion process but relaxed the assumption of neutrality in their analytical formalism. Figure 1 illustrates their results: that the electrons migrate into the void ahead of the

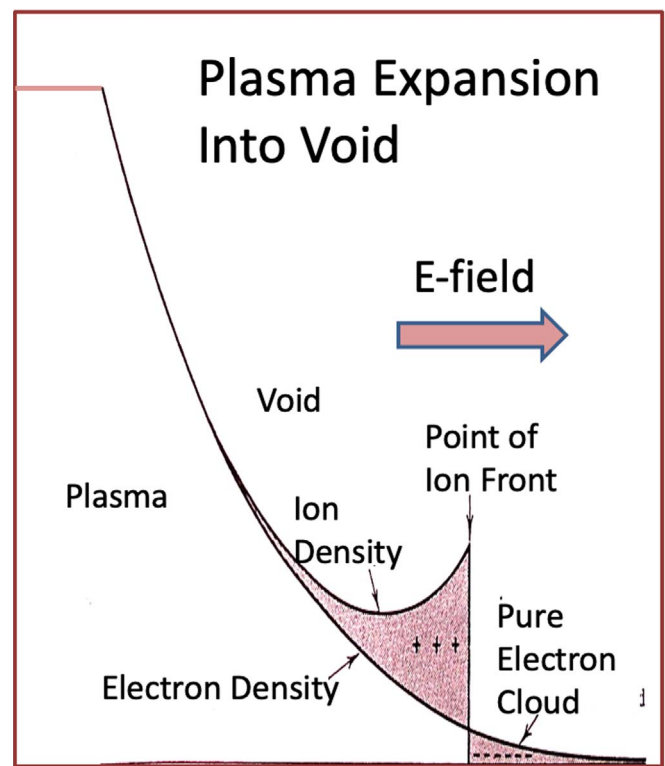


**Figure 1.** Nonneutral wake expansion at the plasma–vacuum interface (figure adapted from Crow et al. 1975).

ions, creating an “electron cloud” region that forms the negative polarity region of a double layer. These electrons are actually the fastest electrons in the solar wind energy distribution (i.e., high-energy tail). Further, because of the  $E$ -field, the ions are accelerated into the void to form an ion beam. This process creates an “ion front” that consists of the fastest group of ions in the expansion. The result of Crow et al.’s analytical approach suggests that a standing double layer—a region where the normally charge-neutral plasma is separated into opposite polarities (predominantly ions spatially adjacent to predominantly electrons)—should form at the earliest times in the plasma expansion process.

Double layers are of general interest in plasma physics, since they represent regions that are not in charge equilibrium, possessing a large cross-layer  $E$ -field and thus an electrical potential drop that is capable of accelerating ions and electrons. For example, double layers have been found in Earth’s auroral regions, creating electron and ion acceleration in the region (Ergun et al. 2004). The idea that the Moon also possesses such a particle acceleration region is intriguing and affirms the view that the plasma environment created by the Moon is a new form of a plasma physics laboratory to examine basic plasma processes.

In order to test whether neutrality is maintained in the wake expansion process as described by Crow et al. (1975), a series of particle-in-cell kinetic simulations were run modeling the wake region near its obstruction along the terminator (Farrell et al. 2008). These particle-in-cell codes do not set  $n_i = n_e$  but allow the ion and electron populations to evolve and be controlled by the electric field that forms in the spatial separation. The interplanetary magnetic field (IMF) in the solar wind in these simulations is assumed to be quasi-perpendicular to the wake flank. As shown in Figure 2, a void

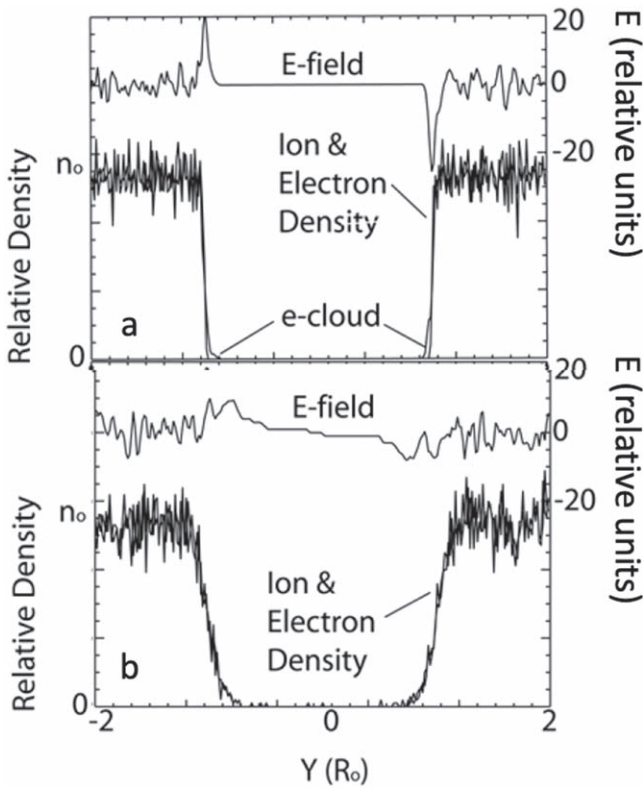


**Figure 2.** Particle-in-cell simulation of the plasma expansion and  $E$ -field behind the Moon for (a) early times in the simulation and (b) later times in the simulation (adapted from Farrell et al. 2008).

in the simulated solar wind plasma is created, and the plasma is allowed to expand into the void along the  $Y$ -direction (same direction as the IMF). As predicted by Crow et al. (1975), at early times in the simulation (Figure 2(a)), the electrons move into the void ahead of the ions to form an electron cloud (labeled “e-cloud” in the figure). The  $E$ -field also has its largest value at the electron cloud interface. At later times in the simulation (Figure 2(b)), the ions have caught up with the electrons. Note that while the simulation is a one-dimensional model of the expansion, the cross-wake profile at each increasing time step represents a position further downstream from the Moon, since the  $Y$ -density profile convects downstream at the solar wind speed,  $V_{sw}$ . The results suggest that there should be a separation of electrons from ions at the plasma–vacuum interface located immediately downstream of the terminator obstruction point. Most likely, this layer changes morphology with the prevailing IMF direction and solar wind conditions, and such changes will also be investigated by TerDLE.

Regarding the size of the nonneutral region, two-dimensional particle-in-cell simulations of the plasma expansion suggest the presence of an extended region. Specifically, Nakagawa’s (2013) simulation found that a nonneutral region forms behind the Moon and has an ion front ( $n_i > n_e$ ) protruding  $\sim 0.2 R_L$  inward from the wake at a downstream distance of nearly  $1 R_L$ . The modeled region is substantially larger than the solar wind Debye length (of  $\sim 15$  m). The finding of an extended nonneutral region is similar that derived in the modified one-dimensional simulations of Farrell et al. (1998, 2008). However, if such an extended nonneutral region existed in downstream regions, it should have been observed

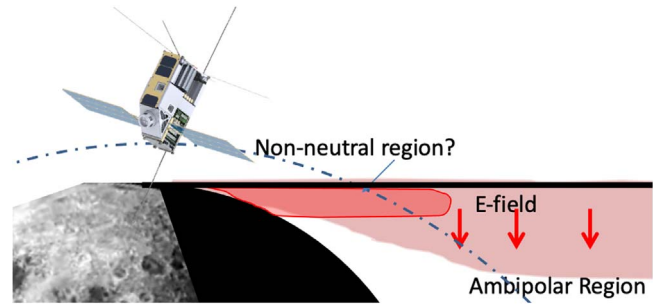


**Figure 3.** Illustration of TerDLE trajectory through the near-Moon expansion region.

and reported by THEMIS-ARTEMIS. While Crow et al. (1975) modeled a nonflowing ion and electron expansion (fluid not convecting downstream), their results can be used to predict the extent of the nonneutral region in its initial stages. Specifically, in Figure 9 of Crow et al. (1975), it is surmised that the nonneutral region near its initiation has a width of  $>100$  Debye lengths (1.5 km) and can propagate downstream at least 50 ion plasma periods ( $>7$  km downstream for a  $400 \text{ km s}^{-1}$  solar wind convection speed). Such a nonneutral region would be at the limit of TerDLE detection, requiring fast sampling at the end of the TerDLE mission. In this more limited case, TerDLE might not detect the nonneutral region but place a well-defined limit on its spatial size.

Two-dimensional particle-in-cell simulations of plasma expansion into regional obstructions, like polar craters, etc., also show the formation of the double layer immediately downstream of the obstruction (Zimmerman et al. 2011, 2012, 2013). These ion sonic wakes and local expansion regions are considered “self-similar” structures (Samir et al. 1983), with the regional mini-expansions being representative of the larger expansion at a global level. Zimmerman et al. (2013) demonstrated analytically and via simulation that a set of recursive regional wakes created by local topography over the terminator merge to form a larger singular and homogeneous wake as the downstream distance progressively increases.

TerDLE specifically targets the plasma–vacuum interface downstream of the terminator to map out electron and ion morphology, examine external controlling influences on the plasma expansion process, and search for and identify the possible electron cloud/double layer regions, if they are present at TerDLE’s altitude. Figure 3 illustrates TerDLE’s passages through the heart of the plasma expansion region.

### 3. Objectives, Significance, and Closure

The plasma expansion region in the near-Moon environment is just beginning to be appreciated as its own unique plasma physics laboratory. Consequently, this special plasma region makes an ideal target for a lunar Cubesat mission. The TerDLE science objectives are as follows.

- (1) Identify any plasma expansion density anomalies at low altitudes near the terminator. In the outer wake regions, spacecraft like Wind and THEMIS-ARTEMIS have demonstrated that the plasma expansion process fits nicely into kinetic simulations of an ion sonic expansion. For example, Xu et al. (2019) mapped the lunar wake potential out to  $4 R_L$  using over 6.5 yr of THEMIS-ARTEMIS data, and the observations were comparable to



a plasma expansion model. However, particle-in-cell plasma simulations suggest that the plasma discontinuity region immediately downstream of the terminator/obstruction has a very complex density structure, possibly even a break in neutrality. The early expansion region may also contain anomalous plasma density fluctuations/plasma waves that have not been observed previously that form at the edges of the flank due to currents associated with the expansion process. Thus, an examination of this region at very low altitudes should be revealing.

- (2) Assess the solar wind's effect on the presence and structure of the wake flank region. The solar wind density, temperature, and magnetic field strength and orientation are all variable in the solar wind, changing on timescales of minutes. The Moon and wake may even undergo changes associated with a passing coronal mass ejection or other extreme space weather event. The type II wakes (Nishino et al. 2010) also represent exceptions to the nominal expansion process. Hence, understanding the nature and structure of the near-Moon expansion region as a function of driving external conditions will further our understanding of the expansion process itself. By its ever-changing nature, the driving solar wind provides opportunities to advance our understanding of the expansion process (i.e., for slow and fast speeds, warm and cold plasma temperatures, varying IMF conditions, etc.). Upstream monitors like Wind and ACE, along with local monitors THEMIS-ARTEMIS, will provide critical information on external environmental conditions.
- (3) Determine if plasma neutrality is maintained or lost during passages through the expansion region. Modeling suggests that the plasma does not maintain neutrality at the wake flank close to the Moon. The size and extent of this nonneutral region remains unknown, and a systematic search for and identification of nonneutral plasma layers has yet to be made. Xu et al. (2019) did report on THEMIS-ARTEMIS passes close to the Moon, presenting statistical analysis from many passes of the electrostatic potential in the near-Moon region. The resolution of the averaging interval closest to the Moon was  $\sim 0.1$  lunar radii, and the potential alone cannot indicate if neutrality is lost, since the potential still varies smoothly across the boundary (see Figure 3 of Crow et al. 1975). TerDLE's instrument complement and unique orbit will allow a search at very low altitudes explicitly examining the differences in  $n_e$  and  $n_i$  to derive the loss of neutrality. It should be noted that this search for the double layer is a primary objective. Also note that the failure to find the double layer does not mean mission failure; instead, TerDLE then provides an upper limit/constraint on the angular width and downstream extent of the double layer. Thus, even a nondetection has value in providing the spatial constraints of the nonneutral region.

Table 1 is the TerDLE science traceability flow from science objectives to mission and instrument requirements to science closure. The methodology for determining the electron cloud/double layer is simple: to compare the measured electron-to-ion density difference  $n_e - n_i$ , as well as the variations in the slope of the densities  $dn_e/dx$  and  $dn_i/dx$  (which removes relative offsets).

Mission requirements include moving from a high-speed hyperbolic orbit imparted at CubeSat ejection into a captured

elliptical lunar orbit with a decreasing periselene at the terminator; this is in order to map out the structure of the near-Moon expansion regions. By the nature of the orbit design, TerDLE will be on orbit for months and will obtain a large statistical set ( $>100$ ) of wake flank crossings under varying solar wind conditions. The wake flank region is a relatively easy target for study, since it is fixed in local time and will be transited twice per orbit by TerDLE.

In examining the measurement requirements in Table 1, one could easily assume an ideal sensor for directly measuring plasma densities is a Langmuir probe, which has had great success operating in the dense Enceladus plasma torus and Titan ionosphere. However, such probes lose sensitivity in low densities (below about  $10 \text{ cm}^{-3}$ ), since they cannot collect enough plasma current at the sensor head to detect the low densities and flux levels expected in the lunar plasma wake near  $0.01 \text{ cm}^{-3}$ . Consequently, we build an “effective” Langmuir probe using a set of complementary sensors: an IS to obtain  $n_i$  and a PWS operating from 0.01 Hz to 100 kHz to measure very low frequency (VLF)  $E$ -fields and  $n_e$  from the intense emission at the electron plasma frequency,  $f_{pe}$ . While an electron spectrometer would obtain the energy character of the electrons, such instruments are highly susceptible to negative spacecraft charging, like that expected in the shadowed wake, which could then potentially create an undercalculation of the  $n_e$  moment. In contrast, the observation of the electron plasma frequency  $f_{pe}$  emission allows for a direct, high-resolution measurement of  $n_e$ .

The TerDLE IS and PWS can provide an accurate measure of  $n_e$  and  $n_i$ , enabling a systematic study of the region downstream of the obstructed flow. The gradient in density,  $dn_e/dx$  and  $dn_i/dx$ , can also be derived and may even be more robust against any systematic offsets in the direct measurement of the density (although it possibly adds noise, depending upon the fluctuations in the values). Besides the  $f_{pe}$  emission, other plasma waves could also be detected at and near the boundary crossing, like broadband electrostatic noise (Farrell et al. 1997). Using  $n_e$ ,  $n_i$ ,  $dn_e/dx$ ,  $dn_i/dx$ , and plasma waves, investigators can examine the character of the wake formation region near the obstacle location and determine if neutrality is lost. This data analysis approach specifically addresses the closure of the first and last science objectives in the traceability matrix in Table 1.

External conditions will alter the nature of the expansion, and monitors like ACE, Wind, and THEMIS-ARTEMIS can be used to correlate the morphology of the expansion with driving conditions. Investigators can then correlate the key TerDLE parameters with prevailing space environmental conditions to determine if a systematic effect is observed. Correlations of wake  $n_e$ ,  $n_i$ ,  $dn_e/dx$ ,  $dn_i/dx$  and plasma waves as a function of driving solar wind and IMF can be made. This data analysis approach specifically addresses the closure of the second science objectives in the traceability matrix in Table 1.

#### 4. TerDLE Instrumentation

Since the CubeSat has limited payload carrying capability, only two instruments were chosen to be on board: the IS and PWS. Both systems were expected to be built at NASA Goddard Space Flight Center. The IS heritage is drawn in part from the flight-proven FASTSAT and VISIONS MINI-ME neutral atom spectrometer (Rowland et al. 2011; Collier et al. 2015). Figures 8 and 9 of Rowland et al. (2011) display the MINI-ME energetic neutral system, with the system following

**Table 1**  
The TerDLE Science Traceability Matrix (STM)

Science Objective	Measurement Requirements	Instrument Requirements	Science Closure	Mission Requirements (Applies to All Objectives)
Identify any plasma expansion density anomalies at low altitudes near the terminator.	Measure $n_e$ and $n_i$ during terminator crossings (LT 6 and $18 \pm 0.5$ hr); measure close to Moon ( $<50$ km).	$n_i$ : 10–0.01 $\text{cm}^{-1}$ , 20–5000 eV. VLF E: 0.01–100 kHz; $>0.01$ $\text{mV m}^{-1}$ providing $n_e$ from $<0.001$ to $123 \text{ cm}^{-1}$ . Sampling on 1 s timescales.	Obtain $n_i$ , $n_e$ , and plasma waves and observe plasma–vacuum discontinuity morphology as obstruction point is approached.	Periselene at low altitudes in vicinity of terminator obstruction point. Orbit to have progressively reducing periselene to below 100 km.
Assess the solar wind’s effect on the presence and structure of the near-Moon expansion region.	Correlate expansion characteristics with prevailing IMF and solar wind conditions.	$n_i$ : 10–0.01 $\text{cm}^{-1}$ , 20–5000 eV. VLF E: 0.01–100 kHz; $>0.01$ $\text{mV m}^{-1}$ providing $n_e$ from $<0.001$ to $123 \text{ cm}^{-1}$ . THEMIS-ARTEMIS or upstream monitors to get SW and IMF.	Derive plasma expansion process under varying external IMF and SW conditions; determine if there are periods when DL disappears; observe other unusual wake types (like type II wakes reported by Kaguya).	Point directly into solar wind flow once per $\sim 10$ s interval. Multiple crossings for months with varying SW conditions.
Determine if plasma neutrality is lost during passages through the ambipolar region.	Create $n_i - n_e$ and $dn_e/dx$ , $dn_i/dx$ profiles to determine if there are consistent differences between these profiles.	$n_i$ : 10–0.01 $\text{cm}^{-1}$ , 20–5000 eV. VLF E: 0.01–100 kHz; $>0.01$ $\text{mV m}^{-1}$ providing $n_e$ from $<0.001$ to $123 \text{ cm}^{-1}$ .	Compare profiles of $n_e$ and $n_i$ to determine if Crow’s electron cloud and ion front are observable; close out this fundamental issue.	No predefined inclination required.

the conversion surface to be used as the TerDLE ion detection system (with a reverse in polarity). For TerDLE applications, the head of the ion instrument that samples the local plasma environment consists of deflectors and two nested toroids. A microchannel plate stack detects ions that have the correct energy to transverse the gap between the toroids based on the applied stepped voltage between the toroids. The TerDLE/IS and all associated electronics were to fit within a 1U segment of the 6U CubeSat. The IS energy range covers 20–5000 eV, and its field of view about the central observing plane was expected to be 360° azimuthally and 10° latitudinally. However, added deflectors would then allow sampling of the ion distributions from about 30° to 45° above the central field-of-view plane, depending on ion energy.

The PWS was planned to be a digital electric radio that operates from 0.01 Hz to 100 kHz. The radio consisted of a deployable antenna of ~1 m length that drives a VLF pre-amp. The pre-amp system is a slight modification of the low-noise VLF amp built for the DSX search coils that have been in orbit in the radiation belts since mid-year 2019 (Scherbarth et al. 2009). The signal is digitized immediately behind this pre-amp, and the remainder of the radio is a digital FPGA system that performs digital filtering and spectral analysis. The primary outputs are wave spectra that will allow a determination of the  $f_{pe}$  peak emission and thus the electron density. The  $f_{pe}$  emissions are stimulated by wake-created plasma instabilities (Bale et al. 1997).

## 5. Mission Implementation as an Artemis-1 CubeSat

The original TerDLE concept was a 12 kg/6U CubeSat that was proposed to be deployed during the flight of the Artemis-1 mission. The TerDLE ion propulsion is low-thrust (<1 mN); thus, the baseline transfer and lunar capture are very similar to the two-phase capture orbit of Lunar IceCube. Lunar IceCube is a selected mission to be deployed on the upcoming Artemis-1 flight. The low-thrust trajectory incorporates a dynamical system (manifold) analysis similar to that used for the capture of the two THEMIS-ARTEMIS spacecraft. One such trajectory analysis representative of the transfer and capture process for Lunar IceCube is illustrated in Figure 7 of Clark et al. (2017). TerDLE and Lunar IceCube have similar heritage (identical spacecraft builders, 6U/12 kg CubeSats, Artemis-1 payloads, similar orbit designs). We thus will reference Lunar IceCube in the TerDLE mission implementation herein, since it is now manifested to fly on Artemis-1.

In Phase 1, TerDLE was initially to be injected into a hyperbolic orbit from the fast-moving interim cryogenic propulsion stage (ICPS) bus of Artemis-1. Direct injection into orbit about the Moon is not possible with the low-thrust system. Instead, upon ICPS release, the CubeSat would apply a modest thrust to target a lunar gravity assist that results in a ballistic transfer trajectory designed to encounter the Moon at a lower velocity. The postlunar flyby energy would be reduced to that of a typical Sun–Earth/Moon system heteroclinic (Earth–Moon captured) manifold. TerDLE then would proceed in a long-duration orbit including a series of Earth periapses to allow long-duration application of the thruster system. The combination of the orbit orientation, Earth periapses, and long-term thruster firings thus allows TerDLE to slow down for lunar capture (see Figure 7 of Clark et al. 2017 as an example of this capture). In effect, the thrust operations and the multibody dynamics are used to raise TerDLE’s Earth orbit

perigee to match a lunar orbit radius, adjust the timing of the lunar encounter, rotate the orbital line of apsides, and achieve a ballistic lunar encounter that reduces or eliminates lunar capture delta-V requirements. We note that each transfer and capture trajectory scenario is robust but highly unique to the specific launch date, Earth–Moon–Sun position, and release speed of the spacecraft. This transfer and capture phase is expected to take 50–100 days, depending upon the launch date and injection speed.

In Phase 2, TerDLE, captured in a highly elliptical lunar orbit, would use the low-thrust system for many days each orbit to progressively reduce the aposelene. This phased thruster use places the spacecraft into its final science orbit having a periselene altitude well below one lunar radius. In the TerDLE orbit design, the thruster sequencing was such that the periselene would vary in altitude, with a periodically occurring minimum periselene value that would progressively drop in altitude to values well below 100 km. Also, the elliptical orbit allows a comparison of the near-surface wake at periselene to that further downstream intercepted at aposelene. The orbit design was such that near the end of the mission, TerDLE would make a set of very low altitude periselene passes at and just nightside of the terminator—locations just downstream of the wake initiation region.

It was planned that the TerDLE CubeSat for the Artemis-1 mission would be built at Morehead State University (MSU), leveraging the team’s substantial and significant CubeSat system engineering and mission experience. The TerDLE development utilizes systems with significant LEO flight heritage and incorporates new nanosatellite technologies to develop an evolved, radiation-tolerant 6U CubeSat bus designed to support interplanetary investigator science. The MSU 6U deep space CubeSat possesses high power generation (for Lunar IceCube, 120 W of continuous power); a radiation-tolerant, distributed multiple processor-based payload processor system; a highly capable miniaturized guidance/nav system designed for lunar missions; an innovative propulsion system; and a high throughput X-band communication system for lunar CubeSat missions.

The 6U CubeSat bus structure is based on a robust two-wall structure matched to central mounting frames and capped by robust, milled bulkheads on the +Z and –Z faces. Subsystem enclosures and braces reinforce the structure throughout the length of the body, allowing the frame to hold very tight tolerances. The design also provides the rigidity required to maintain integrity during vibration. The structure is simple to manufacture and assembles easily during test and integration. The open-sided concept provides easy access to subsystems for systems testing, improves thermal control, and is designed to meet NASA spacecraft venting standards. It serves as a chassis to accommodate four deployable solar panels, four deployable blade antennas, patch antennas, PWS antennas, a thermal management system, and an electromechanical deployment system that stows and controls the deployments in compliance with the NASA launch system provider secondary payload deployment restrictions. The structure has a flight heritage and has consistently passed environmental testing (including vibration and thermal-vacuum) at 3 dB above the NASA Goddard environmental standards.

The MSU bus would integrate key components from expert partners. For Lunar IceCube, these partners include Blue Canyon Technology for the attitude control system, Pumpkin

Inc. for custom solar panels, Busek for ion drive propulsion, and JPL for the Iris  $x$ -band comm system. Like for Lunar IceCube, TerDLE was designed with multiple processors for redundancy. The C&DH architecture was intended to be distributed between the flight computer (Space Micro Proton Lite radiation-tolerant processor), avionics controller (XB1 C&DH), and the low-cost, radiation-tolerant, high-speed payload processor (Honeywell Dependable Microprocessor). Each of the three processing systems would thus have the capability to control basic spacecraft functions, providing redundancy for risk mitigation.

Unlike Lunar IceCube, TerDLE was to utilize a micro-cathode arc thruster micropropulsion subsystem that is an outgrowth of George Washington University (GWU) Micropropulsion and Nanotechnology Laboratory research in scalable small spacecraft electric propulsion. The system would provide  $>600 \mu\text{N}$  of thrust and a total  $\Delta V > 870 \text{ m s}^{-1}$ , levels consistent with the low-energy baseline transfer and capture scenarios described above. The GWU team continues to successfully advance microthrust technology (see Zolotukhin et al. 2020).

The communication approach was to utilize a JPL Iris X-band transceiver coupled to broad-beam patch antennas and a direct-to-Earth transmission to the high-gain MSU 21 m ground station that is now an affiliated node on the NASA Deep Space Network (Deep Space Station 17). The proposed mission operations strategy will support a data throughput rate of a minimum of 128 kbs and ensure the acquisition of 16M samples of data per day—more than enough to meet the science objectives.

## 6. Discussion and Conclusions

TerDLE was designed to target wake flanks that have electrons migrating into the void ahead of the ions, thereby creating an expansion  $E$ -field that is oriented to accelerate ions toward the center of the wake. However, there are other anomalous wake configurations that TerDLE can detect, like the PGR discovered by the Kaguya spacecraft (Nishino et al. 2010). While the conventional wisdom used to be that 100% of the solar wind ions are absorbed on the lunar dayside, Kaguya and Chandrayaan-1 observations (Saito et al. 2008; Lue et al. 2011) suggest that anywhere from 1% to 50% of the incoming protons are reflected from the surface or near-surface magnetic anomalies. Further, these reflected protons maintain substantial energy upon reflection from the dayside magnetic anomalies ( $\sim 80\%$  of incoming energy). Some fraction of these dayside scattered ions will then undergo cyclotron motion in the IMF that carries their trajectories directly into the central lunar nightside/wake region to form a positive proton region called a PGR (Nishino et al. 2010; Xu et al. 2020). This anomalous clustering of positive protons in the central wake then accelerates electrons from the flanks into the wake in order to maintain plasma neutrality. In this case, the expansion  $E$ -field is directed opposite to nominal orientation, with the  $E$ -field directed outward from the central wake region (see Figure 3 of Nishino et al. 2010; Figure 1 of Xu et al. 2020) in order to accelerate the electrons. This proton-dominated wake region was found in about 5%–10% of lunar wake transits (Nishino et al. 2010). TerDLE will examine this region as well at very low altitudes at the wake edge.

The initial TerDLE embodiment was a 6U/12 kg CubeSat, which is a rather limited concept. However, the concept fit into

a scope consistent with the solicitation (the ride and costs). The 2014 H-TIDeS proposal evaluation indicated there were four major strengths to TerDLE: (1) the topic of plasma expansion into a vacuum was a fundamental plasma process worthy of study, (2) the instruments selected could deliver the measurements needed to close Objectives 1 and 2, (3) the proposal demonstrated a feasible mission and lunar orbit insertion scenario, and (4) the proposal demonstrated a mature CubeSat bus. The two major weaknesses were similar in nature, involving a lack of description of (1) instrument capabilities and (2) the required instrument accuracy to uniquely identify the non-neutral region to thus close Objective 3. The concern was that the electron and ion density differences might be so subtle as to be indistinguishable as measured. As described above, kinetic simulations like that in Figure 2 and Nakagawa (2013) find that the nonneutral region just inward of the wake flank has a measurable density difference in an extended region that is detectable. However, analytical models of the expansion (Crow et al. 1975) suggest that the region could be small in extent. At this point, the size and extent of a nonneutral double layer is currently unknown, and this is why TerDLE will perform a search (Objective 3). However, if it is ultimately found that the difference in density is not resolvable by the TerDLE instrumentation, that result also will be reported as an upper limit to the electron and ion density difference (and thus an upper limit of the spatial extent of the double layer structure) during the near-terminator overflights. Hence, a nondetection by TerDLE is still a reportable result.

In an updated version of TerDLE, the same science objectives can be achieved by any larger spacecraft with an IS and PWS passing in close proximity to the near-Moon wake flank. Thus, the science target could be achieved by a large spacecraft proposed under the NASA SIMPLEX program, which allows for larger bus sizes with expanded funding envelopes. A larger spacecraft could also include an electron spectrometer. As shown by Halekas et al. (2005), the electron energy distribution at high energies measured in the wake region provides a direct measure of the plasma expansion potential. In this application, the wake electron energy distribution systematically shifts to lower energies compared to the energy distribution in the free-flowing solar wind. The energy shift is a direct measure of the wake potential. Unfortunately, electron spectrometer systems are sensitive to the negative spacecraft charging expected in shadowed regions, which would affect (reject) the lower-energy electron population. However, the use of an electron spectrometer as a potential probe as derived by the higher-energy electron population would provide added information on the wake flank.

Another possible inclusion to a TerDLE-like concept on a larger bus is a measure of the DC  $E$ -field. Such a sensitive system is currently part of the FIELDS package on board the Parker Solar Probe (Bale et al. 2016). Mozer et al. (2020) measured the  $E$ -field near the Sun at  $<2 \text{ mV m}^{-1}$  (to derive a Poynting flux,  $EB/\mu_0$ , of  $<2 \times 10^{-4} \text{ W m}^{-2}$  in a 100 nT  $B$ -field). The DC  $E$ -field would then provide a direct measurement of the solar wind convection  $E$ -field and possibly the added effect of the expansion  $E$ -field, although the latter is near the limit of detection (and possibly remains below  $1 \text{ mV m}^{-1}$ ; see Figure 5 of Holmström et al. 2012).

Another addition to the payload is a magnetometer. It is well known that diamagnetic currents flow along the wake flank,



and these currents can be sensed by the associated perturbation in the magnetic field (Owens et al. 1996; Halekas et al. 2005). Alfvén wing currents (Zhang et al. 2016), Mach cone boundary currents, and rarefaction currents (Fatemi et al. 2013) are also generated by the Moon–solar wind interaction. It would be interesting to know if there are more complex current structures associated with disturbed particle populations in locations that have nonneutral expansion fronts. If so, one could search for a correlation between anomalous magnetometer-sensed currents and plasma wave activity as sensed by the PWS.

A key requirement is passing through the near-Moon wake flank at the lowest possible altitude. As described previously, we expect the expansion front to be a near-perfect discontinuity just behind the terminator. In regions downstream, we then expect the electron cloud and double layer to form. One possible way to consistently get to very low altitudes ( $<20$  km) is the use of a dual-spacecraft tethered satellite system like that described by Collier et al. (2016). While the center of gravity for the tethered pair can be 50 km, one spacecraft can be located at much lower altitudes, allowing a sensing of the time-stationary expansion structure just a few kilometers downstream of its terminator obstruction location on nearly every orbital transit. In fact, in a SIMPLEX call, one can imagine flying a dual TerDLE, with one CubeSat at very low altitudes passing through the wake region just downstream of the terminator. A “tethered TerDLE” would be an exciting future mission.

To summarize, we describe the TerDLE mission to examine the formation region of the trailing lunar wake that forms in the solar wind plasma flowing antisunward from the Moon. TerDLE is designed to search the near-Moon wake flank region for unusual plasma structures, derive solar wind–driven wake variability, and search for regions where plasma neutrality is lost (double layers). Immediately downstream of the terminator, it is anticipated that a near-perfect plasma discontinuity forms, with solar wind on one side and a void on the other. Simulations show that the first action is to have low-mass electrons of larger thermal velocity move into the void before the heavier protons, creating a local loss of neutrality. The downstream extent of this nonneutral region (i.e., double layer) is currently unknown, but TerDLE can either define or place limits on the nonneutral region’s extent. While the initial TerDLE concept was proposed as a CubeSat for the Artemis-1 mission, we present other embodiments that include an expanded payload beyond the IS and PWS. We also describe a future tethered TerDLE mission to consistently obtain low-altitude flybys over the terminator regions where the plasma expansion is initiated.

We gratefully acknowledge funding from SSERVI and the LEADER Center for Space Environments in the preparation of this manuscript.

## References

- Angelopoulos, V. 2011, *SSRv*, **165**, 3
- Bale, S. D., Goetz, K., Harvey, P. R., et al. 2016, *SSRv*, **204**, 49
- Bale, S. D., Owen, C. J., Bougeret, J.-L., et al. 1997, *GeoRL*, **24**, 1427
- Bonnell, J. W., Mozer, F. S., Delory, G. T., et al. 2008, *SSRv*, **141**, 303
- Bosqued, J. M., Lormant, N., Reme, H., et al. 1996, *GeoRL*, **23**, 1259
- Clack, D., Kasper, J. C., Lazarus, A. J., Steinberg, J. T., & Farrell, W. M. 2004, *GeoRL*, **31**, L06812
- Clark, P., Malphrus, B., Reuter, D., et al. 2017, *Proc. SPIE*, **9978**, 99780C
- Collier, M. R., Chornay, D., Clemmons, J., et al. 2015, *ASR*, **56**, 2097
- Collier, M. R., Vondrak, R. R., Hoyt, R. P., et al. 2016, *AcAau*, **128**, 464
- Crow, J. E., Auer, P. L., & Allen, J. E. 1975, *JIPh*, **14**, 65
- Ergun, R. E., Andersson, L., Main, D., et al. 2004, *JGRA*, **109**, A12220
- Farrell, W. M., Fitzenreiter, R. J., Owen, C. J., et al. 1996, *GeoRL*, **23**, 1271
- Farrell, W. M., Kaiser, M. L., & Steinberg, J. T. 1997, *GeoRL*, **24**, 1135
- Farrell, W. M., Kaiser, M. L., Steinberg, J. T., & Bale, S. D. 1998, *JGR*, **103**, 23653
- Farrell, W. M., Stubbs, T. J., Halekas, J. S., et al. 2008, *GeoRL*, **35**, L05105
- Farrell, W. M., Tribble, A. C., & Steinberg, J. T. 2002, *JSpRo*, **39**, 749
- Fatemi, S., Holmström, M., Futaana, Y., Barabash, S., & Lue, C. 2013, *GeoRL*, **40**, 17
- Halekas, J. S., Angelopoulos, V., Sibeck, D. G., et al. 2011, *SSRv*, **165**, 93
- Halekas, J. S., Bale, S. D., Mitchell, D. L., & Lin, R. P. 2005, *JGRA*, **110**, A07222
- Halekas, J. S., Poppe, A. R., Delory, G. T., et al. 2012, *JGRE*, **117**, E06006
- Halekas, J. S., Poppe, A. R., & McFadden, J. P. 2014, *JGRA*, **119**, 5133
- Holmström, M. S., Fatemi, S., Futaana, Y., & Nilsson, H. 2012, *EP&S*, **64**, 237
- Lue, C., Futaana, Y., Barabash, S., et al. 2011, *GeoRL*, **38**, L03202
- McFadden, J. P., Carlson, C. W., Larson, D., et al. 2008, *SSRv*, **141**, 277
- Mozer, F. S., Apapitov, O. V., Bale, S. D., et al. 2020, *ApJS*, **246**, 68
- Nakagawa, T. 2013, *JGRA*, **118**, 1849
- Ness, N. F. 1972, in *Solar Terrestrial Physics 1970*, ed. E. R. Dyer (New York: Springer), 159
- Ness, N. F., Behannon, K. W., Taylor, H. E., & Whang, Y. C. 1968, *JGR*, **73**, 3421
- Ness, N. F., & Schatten, K. H. 1969, *JGR*, **74**, 6425
- Nishino, M. N., Fujimoto, M., Saito, Y., et al. 2010, *GeoRL*, **37**, L12106
- Ogilvie, K. W., Steinberg, J. T., Fitzenreiter, R. J., et al. 1996, *GeoRL*, **23**, 1255
- Owens, C. J., Lepping, R. P., Ogilvie, K. W., et al. 1996, *GeoRL*, **23**, 1263
- Poppe, A. R., Fatemi, S., Halekas, J. S., Holmström, M., & Delory, G. T. 2014, *GeoRL*, **41**, 3766
- Rowland, D. E., Collier, M. R., Sigwarth, J. B., et al. 2011, in *IEEE 2011 Aerospace Conf. (Piscataway, NJ: IEEE)*
- Saito, Y., Yokota, S., Tanaka, T., et al. 2008, *GeoRL*, **35**, L24205
- Samir, U., Wright, K. H., Jr., & Stone, N. H. 1983, *RvGeo*, **21**, 1631
- Scherbarth, M., Smith, D., Adler, A., et al. 2009, *Proc. SPIE*, **7438**, 74380B
- Schubert, G., & Lichtenstein, B. R. 1974, *RvGSP*, **12**, 592
- Spreiter, J. R., March, M. C., & Summers, A. L. 1970, *CosEI*, **1**, 5
- Tribble, A. C. 1988, PhD thesis, Univ. Iowa
- Tribble, A. C., Pickett, J. S., D’Angelo, N., & Murphy, G. B. 1989, *P&SS*, **37**, 1001
- Xu, S., Poppe, A. R., Halekas, J. S., et al. 2019, *JGRA*, **124**, 3360
- Xu, S., Poppe, A. R., Halekas, J. S., & Harada, Y. 2020, *JGRA*, **125**, e28154
- Zhang, H., Khurana, K. K., Kivelson, M. G., et al. 2014, *JGRA*, **119**, 5220
- Zhang, H., Khurana, K. K., Kivelson, M. G., et al. 2016, *JGRA*, **121**, 10698
- Zimmerman, M. I., Farrell, W. M., & Stubbs, T. J. 2013, *Icar*, **226**, 992
- Zimmerman, M. I., Farrell, W. M., Stubbs, T. J., Halekas, J. S., & Jackson, T. L. 2011, *GeoRL*, **38**, L19202
- Zimmerman, M. I., Jackson, T. L., Farrell, W. M., & Stubbs, T. J. 2012, *JGRE*, **117**, E00K03
- Zolotukhin, D. B., Daniels, K. P., Brieda, L., & Keidar, M. 2020, *PhRvR*, **102**, 021203